 https://doi.org/10.3311/PPci.36949


**Periodica Polytechnica Civil Engineering**, 68(4), pp. 1268–1280, 2024

# Failure Mechanism and Structural Optimization of the Primary Support Structure for Expressway Tunnel in Soft Rock: A Case Study

Yamin Wu[1,2*], Junfeng Duan[1], Jinfeng Xu[2], Wanmin Xu[3]

[1] Department of Architecture Engineering, Zhengzhou University of Industrial Technology, 100 Science Avenue, Zhengzhou 451100, Henan, China
[2] College of Civil Engineering, Tongji University, 1239 Siping Road, Shanghai 200092, China
[3] Yunnan Jiaotou Highway Construction Sixth Engineering Co., 37 Qianxing Road, Kunming 650228, China
[*] Corresponding author, e-mail: WUyamin@zzuit.edu.cn

Received: 24 March 2024, Accepted: 24 May 2024, Published online: 08 July 2024

**Abstract**

When the highway tunnel crosses the soft rock, the primary support structure often fails and damages because it cannot withstand the excessive surrounding rock pressure. For the Magu tunnel in Yunnan Province, which is in the upper hard and lower soft stratum, the surrounding rock deformation is large, and the primary support structure occurs spray concrete cracking, steel arch frame twisting deformation. According to the convergence constraint curve, this paper proposes to adopt the primary support optimization design scheme of "shortening the bench length + optimizing the length and arrangement of anchor rods". According to the numerical simulation results of FLAC3D, the important indexes such as deformation convergence, surrounding rock stress, anchor axial force and thickness of plastic zone in different excavation support conditions are analyzed. The conclusions are as follows: 1. The soft rock at the foot of the benches does not provide sufficient support resistance, resulting in large settlement and convergence deformation that can cause the primary support structure to fail and become damaged. 2. The length of the middle bench and the primary support strength and stiffness contribute most to the deformation. 3. The deformation control effect of the short anchor rods on the surrounding rock is relatively weak. Increasing the length of anchor can better play the role of anchor suspension enhancement and give full play to the surrounding rock's own bearing capacity. Finally, the deformation of the tunnel is under control after adopting the optimized primary support structure, which ensures the smooth construction.

**Keywords**

tunnel engineering, primary support structure, structural optimization, mechanical properties, failure mechanism analysis

## 1 Introduction

In recent years, China's tunnel construction has made great progress in construction technology, quality control and service level have stepped up to a new level, and there are mature excavation methods and support means for tunnel construction in different geological conditions [1, 2]. However, tunnel excavation often encounters special geological conditions, in which composite strata as a representative of the adverse geological conditions, many scholars from different perspectives to put forward the corresponding countermeasures. Some scholars believe that tunnel excavation in complex strata should be dynamically adjusted to determine the optimal parameters after excavation by means of information technology such as monitoring and measuring [3–5]. In addition, considering the complexity of the upper hard and lower soft strata, the stability of the surrounding rock should be fully utilized. The rapid construction method of installing additional system anchors in the middle and lower benches, supporting the tunnel as it is excavated, closing the inverted arch into a ring in time, and following the lining closely effectively improves the construction progress and ensures the construction safety [6, 7].

Anchor rods are an effective means of support measures for controlling the deformation of the surrounding rock in tunnels with complex strata [8–10]. The combination of long and short anchors is useful for controlling the deformation of surrounding rock at the top. High strength locking anchors are beneficial to stabilize the foot of a

**Cite this article as:** Wu, Y., Duan, J., Xu, J., Xu, W. "Failure Mechanism and Structural Optimization of the Primary Support Structure for Expressway Tunnel in Soft Rock: A Case Study", Periodica Polytechnica Civil Engineering, 68(4), pp. 1268–1280, 2024. https://doi.org/10.3311/PPci.36949

vault, and according to the existing studies, it is known that when the insertion angle of locking anchors is in the range of 15°~20°, it has the strongest controlling effect on the deformation of the surrounding rock [11, 12]. Besides, it is more effective to reduce the convergent deformation of the tunnel by increasing the anchor density than by increasing the anchor length. Under the condition of conventional anchor arrangement parameters, the reduction of final tunnel convergence by anchor support will not exceed 20%. For prestressing anchors, increasing the initial anchor force for end anchors is beneficial for anchor control of anchor solids, while the effect is not obvious for full bounded anchors, where the main role of initial anchors is to increase the compressive strength, cohesive force and internal friction angle of the rock mass [13–15]. For full-length anchors, some researchers had concluded that the main form of damage is the slip failure between the anchor and the anchoring agent, and suggested increasing the strength of the anchoring agent and avoiding the use of anchors with a small radius [16–18].

In addition, many scholars have shown that for deformation control of tunnel bench method construction, reasonable control of bench length, bench height and excavation footage per cycle can effectively reduce tunnel over-excavation and excavation disturbance. By adjusting the primary support parameters of the upper and middle benches, the release of surrounding rock stress and tunnel deformation control can be achieved [19]. Finally, many scholars have achieved certain research results on the field application and engineering effects of primary support structures in soft rock tunnels [20–22]. However, many studies mainly rely on the field tests with high cost. Numerical calculations provide an effective analytical tool for the study of the interaction between the tunnel envelope and the initial support.

The above scholars have fully studied and given targeted advice on the excavation methods, means of support and deformation control of tunnels under different geological conditions. However, tunnels are located in a wide variety of geological environments, and case studies of tunnels constructed by the New Austrian Tunnelling Method (NATM) in rare geological formations, especially in the upper-hard-lower-soft stratigraphic conditions, are extremely rare. Therefore, based on the research of the above scholars, this paper relies on the Magu Tunnel of Mengmeng Expressway in Yunnan Province to carry out the optimal design of tunnel excavation and initial support scheme for the special soft rock stratum of full, strongly weathered granite mixed rock with hard upper and soft lower strata. To achieve the purpose of improving the construction quality, reduce the occurrence of engineering accidents, and provide reference basis for similar projects.

## 2 Engineering geological condition and field testing

### 2.1 Engineering overview

Magu Tunnel is located at the junction of Lincang City and Yunxian County, belonging to the control project of Meng Meng Expressway. The project area is located in the southwestern edge of the Yunnan-Guizhou Plateau, the southern section of the Hengduan Mountain Range, for the Nujiang River and the Lancang River inter-river plots, for the stripping type of low mountainous terrain. The tunnel is a separated tunnel, the width of the tunnel design section is 12.5 m, the height is 10.2 m. The total length of the tunnel is 7.38 km, and the maximum overburden is about 1089 m.

### 2.2 Engineering geological condition and tunnel construction program

The left section of the tunnel exit section, ZK22+250~ZK22+280, is at a depth of about 60 m. The tunnel passes through strata containing strongly weathered granite, fully weathered granite, fault mud and fault breccia. Among them, the mineral composition of the rock layer has a high content of feldspar and mica. In addition, the rock mass is in broken~scattered structure, the surrounding rock mass has no self-stabilizing ability, and it is easy to produce large landslides if the support is not timely installed. The actual excavation exposes the stratum as shown in Fig. 1, the upper half section is grey strongly weathered granite, with more developed structural surface and poor combination between layers.


**Fig. 1** The field geology of the tunnel excavation face

The lower half of the section is yellow fully weathered granite, the rock mass has micro-expansion when it meets water, and rapidly softens and disintegrates. The rock layer demarcation line is roughly at the junction of the lower and middle steps in the original excavation scheme. The excavation surface is overall wet without water dripping, and the overall integrity and self-stabilization of the surrounding rock is poor.

This section of the tunnel was constructed using the three-bench method. The length of the upper bench is 4 m, the height is 3.2 m, and the excavation feed is 1.2 m per cycle. The length of the middle bench is 12 m, the height is 2.8 m, and the excavation feed is 3.6 m per cycle. The length of the lower bench is 4 m, the height is 2.5 m, and the excavation feed is 2.4 m per cycle. After the lower bench is executed, the excavation of the inverted arch and its support will be carried out immediately, and the height of the inverted arch is 1.6 m. After the completion of the excavation of the tunnel and its primary support, the concrete of the inverted arch will be poured immediately.

### 2.3 Damage of the tunnel's original primary support and deformation monitoring

The original primary support adopts SF5a type lining, and the specific support parameters are shown in Table 1. Among them, the reinforcing mesh is to be laid after the initial spraying of 2 cm of concrete on the excavation surface, and the deformation amount reserved for design is 15 cm. The grouting pressure of locking foot anchors is 0.5–1 MPa.

**Table 1** Original primary support scheme of the tunnel

| Support structure | Design parameters |
|---|---|
| Over-head small grouting pipe umbrella | ∅42 × 4 steel pipe, 4.5 m long, ring spacing 30 cm, overlap length 3 m. |
| Primary support | 1. Shotcrete: C25 concrete, 25 cm thick.<br>2. Reinforcing steel mesh: double layer ∅8 mm reinforcing steel mesh with a grid spacing of 15 cm × 15 cm.<br>3.Steel frame: I18 I-beam, 60 cm spacing per joist, longitudinally connected with steel bars, 1 m spacing.<br>4. Inverted arch filler: C15 concrete. |
| Secondary lining | 1. Concrete: C30 waterproof reinforced concrete, 60 cm thick.<br>2. Reinforcing steel: HRB400 steel bar. |
| Anchors | 1. Radial anchor size is ∅25 × 5. Hollow grouting anchor is arranged according to plum blossom shape, spacing 100 × 60 cm (ring × longitudinal), each root is 3 m long.<br>2. The size of ∅42 × 4 small conduit is arranged at the foot of the arch, and the length of each one is 4.5 m. |

During the construction of this tunnel section, the upper bench and middle bench were constructed according to the original primary support scheme, then the deformation convergence was large. During the excavation of the lower bench, because the rock mass at the lower bench position is mainly fully weathered granite, when the lower step support was applied, the surrounding rock fell off seriously and could not be self-stabilized. The peripheral rock in front of the vertical arch showed serious hollowing phenomenon, so the initial support was applied in time and concrete backfill was carried out. During the period of continuous monitoring, the settlement curve of the tunnel arch and the convergence curve of the arch shoulder are shown in Fig. 2.

After blasting and excavation of the upper bench, the deformation rate of the tunnel roof subsidence and the deformation rate of the arch foot of the upper stage were less than 10 mm/d. During the excavation of the middle bench, the rate of tunnel roof subsidence and horizontal

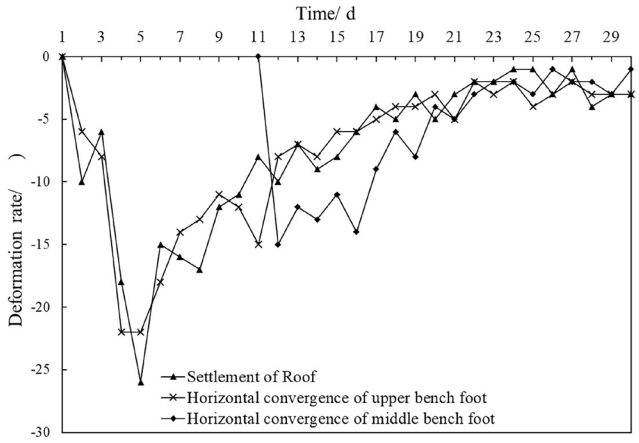


(a)

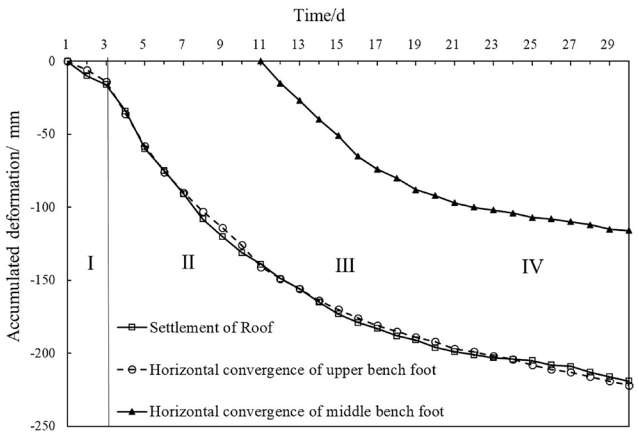


(b)

**Fig. 2** Deformation monitoring of primary support in typical sections of tunnels: (a) Deformation rate at tunnel monitoring points, (b) Accumulated deformation at tunnel monitoring points

convergence rapidly became larger, and the maximum deformation amount of a single day was 26 mm, and the deformation rate of the subsequent tunnel was reduced. After the lower bench, the tunnel roof subsidence and the horizontal convergence rate of the arch shoulder were reduced to below 10 mm/d. However, the deformation time of the surrounding rock was longer. However, the surrounding rock deformation time is long and has not reached a stable convergence state. Fig. 2 (b) shows the cumulative deformation of the tunnel with monitoring time, which is divided into four regions. Region I shows the change of tunnel deformation after the upper bench excavation, when the tunnel deformation is small. Region II is due to the soft rock on the lower side of the arch footing, the arch footing has no reliable support after the primary support is applied in the middle bench, and the locking footing anchors alone cannot bear the upper peripheral rock load. Therefore, this section is the main part of the tunnel deformation convergence. Region III shows the deformation convergence of the lower bench, when the deformation around the tunnel continues to increase. The monitoring results show that the horizontal convergence of the tunnel arch waist is much smaller than the horizontal convergence of the arch shoulder, which is due to a certain amount of over-excavation deformation occurred before the tunnel excavation, while the actual monitoring can only measure the deformation of the tunnel after excavation. Region IV is the deformation convergence during the construction of the inverted arch. With the closure of the ring, the resistance of the primary support to the surrounding rock increases, and the deformation of the tunnel gradually tends to stabilize.

As shown in Figs. 2 and 3, the monitoring results and damage of the primary support show that adopting the original construction program to pass through this section of the tunnel will lead to greater tunnel deformation, which will affect the application of the secondary lining. In addition, many landslides have occurred during the tunnel boring process, and the construction risk is higher, so it is more important to strictly control the deformation convergence around the excavated cavity to prevent possible local subsidence and topping disaster. According to the actual situation on site and the experience of previous projects, it is recommended to adopt the scheme of full-section anchor + optimized step length to pass through this complex geological section. On the other hand, the tunnel deformation convergence is affected

(a)

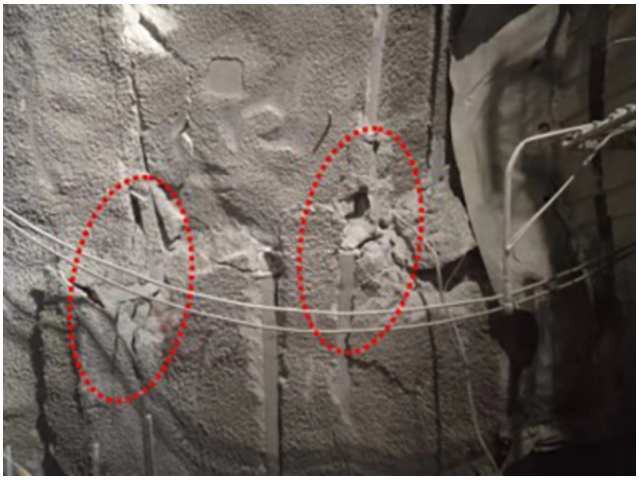

(b)

**Fig. 3** Damage of the original primary support: (a) Localized deformation damage to primary support, (b) Twisted steel arch joints

by the tunnel excavation scale, the smaller the excavation scale is, the smaller the tunnel deformation convergence is [18, 20]. However, the excavation footage of the tunnel is limited by the actual progress of the project and the influence of the design spacing of the steel arch, which cannot be shortened arbitrarily. According to the mechanical characteristics of tunnel construction, the excavation footage of both middle and lower steps were shortened to 1 m, and the spacing of steel arches was reduced to 0.5 m in order to reduce the blasting disturbance and prevent the tunnel from collapsing suddenly. In order to obtain the optimal step length and anchor arrangement scheme, numerical simulation calculations were carried out. And according to the site construction and monitoring conditions for dynamic adjustment, in order to get the optimal construction programs.

## 3 Optimization for bench length

### 3.1 Numerical models and parameters

According to the engineering geological data, the average depth of the tunnel section from ZK22+250 to ZK22+280 is about 60 m. The maximum width of the horseshoe-shaped section of the tunnel is 12.5 m. The upper surrounding rock of the horizontal center line of the tunnel profile in this section is strongly weathered granite, and the surrounding rock in the lower part is fully weathered granite. In this paper, HyperMesh 2021 software is used for geometric modelling and meshing. Subsequently, it was imported into Flac3D 6.0 finite difference numerical simulation software for calculation. Considering that the static influence of the tunnel excavation on the surrounding geotechnical rock mass is generally 3~5 times of the tunnel diameter. In order to eliminate the influence of boundary effect, the length along the tunnel axis (y-axis) is taken as 100 m, and the length along the tunnel transverse (x-axis) and tunnel vertical (z-axis) are both 120 m. The boundary conditions of the numerical model are as follows: fixed constraints at the bottom, horizontal displacements on the left and right sides, longitudinal displacements on the front and back sides, and a free surface at the top. Therefore, the established numerical model is shown in Fig. 4.

The numerical simulation uses the built-in FISH language in Flac3D 6.0 to control the excavation support and parameter assignment of the tunnel step method. Among them, the layered rock mass is simulated with solid units, and the M-C intrinsic model is adopted. The upper 60 m of the model is class IV surrounding rock, and the lower 60 m is class V surrounding rock, which are assigned different physical and mechanical parameters. The initial support is simulated by shell unit, and the linear elasticity constitutive model is selected. The thickness of the initial support is set to be 22 cm. the secondary lining is simulated by solid unit, and the line elasticity constitutive model is selected, and its thickness is 60 cm. the locking anchor and the system anchor are simulated by cable unit. The contact between anchor and lining is set as rigid contact to prevent its end from slipping. A full-length bond is set between the anchor and the surrounding rock to simulate a full length anchored anchor. The length of the locking foot anchor is 4.5 m, and the length of the system anchor is 3 m. The numerical simulation tunnel excavation support model is shown in Fig. 5.

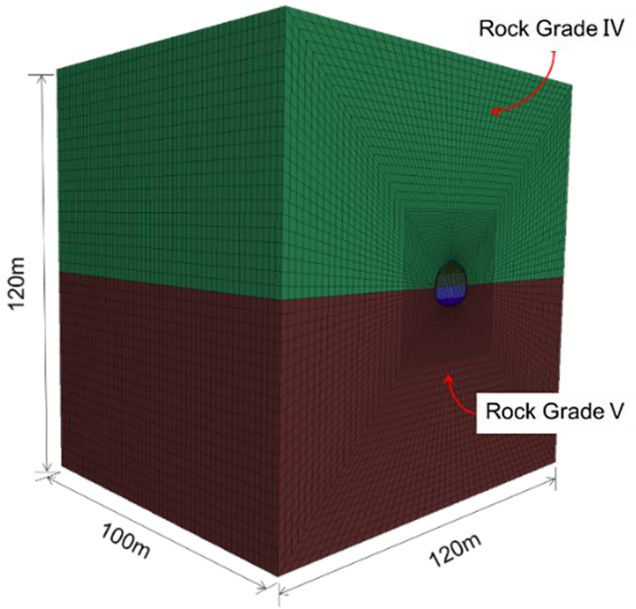


**Fig. 4** Numerical calculation of the overall model for tunnel excavation

The rock and lining structure material parameters are taken in combination with the actual situation, as shown in Table 2. The initial support stiffness is calculated by the principle of equivalent stiffness, and the principle of equivalence is calculated according to formula Eq. (1).

$$E = \left(E_c A_c + E_s A_s\right) / A \tag{1}$$

Where $E$ is the discounted modulus of elasticity of the primary support, $E_c$ is the modulus of elasticity of the shotcrete, $E_s$ is the modulus of elasticity of the I-beam, $A_s$ is the cross-sectional area of the I-beam, and $A_c$ is the cross-sectional area of shotcrete per unit width. The anchor material parameters are shown in Table 3. The anchor is the synonym expression to the "rock bolt".

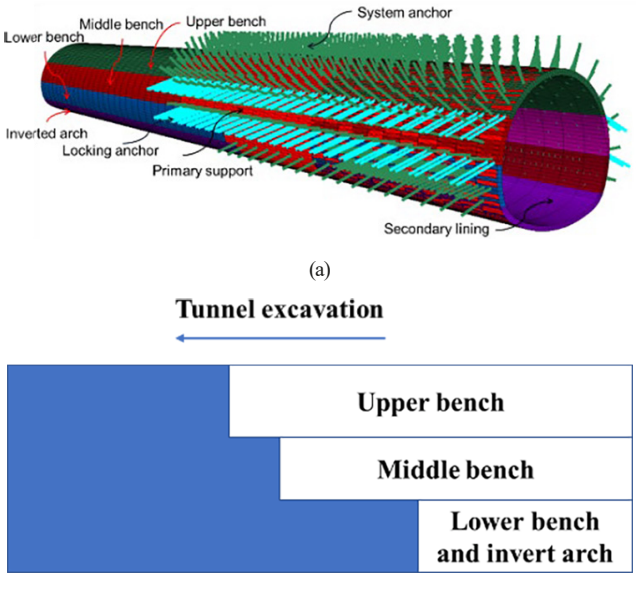


**Fig. 5** (a) The partial numerical model of tunnel excavation and support, (b) Longitudinal schematic of the tunnel excavation

**Table 2** Material parameters of numerical model

| Material | Density/ kN·m$^{-3}$ | *E*/ GPa | Poisson's ratio | Cohesion/ MPa | Internal friction angle/° |
|---|---|---|---|---|---|
| Rock grade IV | 24 | 5.2 | 0.25 | 0.25 | 29 |
| Rock grade V | 23 | 1.5 | 0.28 | 0.1 | 15 |
| Primary support | 22 | 29 | 0.25 | — | — |
| Secondary lining | 22 | 35 | 0.23 | — | — |

**Table 3** Physical parameters of the rock bolt

| Material | *E* | Yield axial force | Slurry cohesion | Slurry stiffness | Slurry friction angle |
|---|---|---|---|---|---|
| | GPa | N | MPa | MPa | ° |
| Locking anchor | 206 | $4.55 \times 10^6$ | 20 | 24 | 45 |
| System anchor | 206 | $4.55 \times 10^6$ | 20 | 24 | 45 |

Considering the influence of the boundary effect on the monitoring results, the tunnel monitoring position is taken at the 50 m longitudinal section of the tunnel. The arrangement of monitoring points is shown in Fig. 6. The monitoring points are arranged at the top of the arch, arch shoulder, arch waist, arch foot and inverted arch positions to monitor the displacement around the hole, internal force and stress of the supporting structure, and axial force of the anchor rods. In addition, the stress distribution of the rock mass within the tunnel anchor arrangement is monitored.

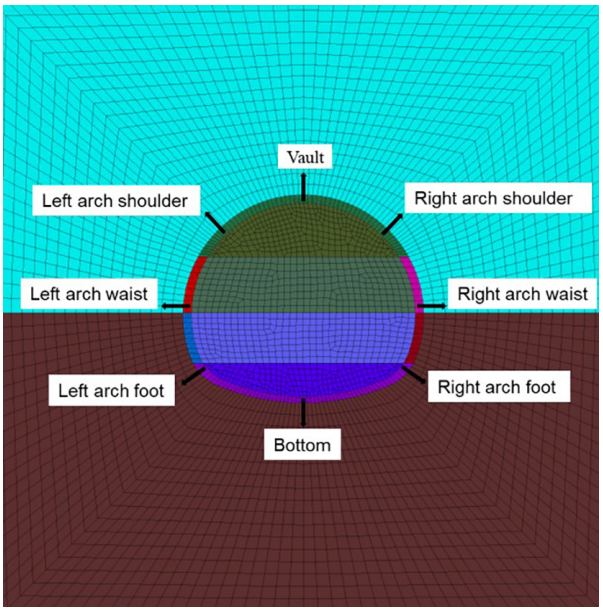


**Fig. 6** Layout of the monitoring points

### 3.2 Numerical calculation design for bench length of different working conditions

The original length of the upper, middle and lower benches of the tunnel is 4 m, 12 m and 4 m respectively, and the height is 3.2 m, 2.8 m and 2.5 m respectively, and the height of the upward arch is 1.6 m. The inverted arch is applied at the same time with the lower step. Due to the upper bench arch needs a certain operation space, and the surrounding rock condition of the upper bench is relatively good. Therefore, the length of the upper bench is not shortened in the numerical simulation. As the arch foot of the middle bench is close to the weak surrounding rock on the lower side of the tunnel, and the actual monitoring data show that the deformation convergence rate of the tunnel is larger during the excavation of the middle bench. Therefore, the reasonable shortening of the middle bench length can reduce the deformation convergence of the tunnel. In addition, previous studies show that, soft rock tunnel arch excavation length should not be greater than 3 m [20]. Therefore, combined with the actual construction progress, shorten the length of the lower bench and the arch to 2 m. This can not only accelerate the primary support closure into a ring, but also reduce the risk of tunnel toppling disaster. Considering the nature of the tunnel surrounding rock and the site construction situation, numerical simulation working conditions (WC) with different bench lengths are set, as shown in Table 4. And control all the working conditions in the secondary lining behind the palm face distance are 30 m. which, WC0 and the original excavation support scheme is the same.

### 3.3 Analysis of calculation results

According to the calculation results, the displacement and stress data of the monitoring points are extracted. The deformation comparison between the numerical simulation control group and the deformation around the hole after excavation of each bench in the actual project is shown in Table 5.

**Table 4** Numerical simulation working condition design of bench length

| Working conditions (WC) | Upper bench length | Middle bench length | Lower bench length | Excavation length | Distance of second lining behind excavation face |
|---|---|---|---|---|---|
| | m | m | m | m | m |
| 0 | 4 | 12 | 4 | 1.2 | 30 |
| 1 | 4 | 12 | 2 | 1 | 30 |
| 2 | 4 | 10 | 2 | 1 | 30 |
| 3 | 4 | 8 | 2 | 1 | 30 |
| 4 | 4 | 6 | 2 | 1 | 30 |
| 5 | 4 | 4 | 2 | 1 | 30 |

**Table 5** Comparison of tunnel deformation in numerical simulation and actual engineering

| Monitoring position | | Circumferential deformation/mm | | |
|---|---|---|---|---|
| | | Before excavation of the middle bench | Before excavation of the lower bench | Final value |
| Settlement of vaults | Actual projects | 2.3 | 14.6 | 22.8 |
| | WC0 | 4.7 | 13.8 | 21.8 |
| Converge of arch waist | Actual projects | 0 | 9.7 | 11.2 |
| | WC0 | 0 | 8.5 | 10.6 |

As the deformation of the tunnel periphery can only be monitored after the primary support is applied in the actual project, the deformation of the tunnel is not considered in the deformation amount of the tunnel's over-arching deformation. Therefore, the deformation convergence value of the tunnel perimeter in numerical simulation is deducted from the amount of overrun deformation and then compared with the actual project, and the deformation convergence of the control group in Table 5 has been deducted from the overrun deformation. From Table 5, it can be seen that the deformation trend of the control group during the excavation process of the step method is consistent with the monitoring results of the actual project. In addition, the size of tunnel deformation convergence in WC0 is also less different from the actual project. Therefore, the design of the parameters in the numerical simulation is more reasonable, and the numerical simulation results can well simulate the actual project.

The tunnel roof settlement data from WC1 to WC5 were extracted and the longitudinal deformation curve of the tunnel was plotted, as shown in Fig. 6. As can be seen from Fig. 7, the final settlement of the tunnel roof is 19.5 cm when the length of the middle bench is 12 m (WC1), and it decreases with the shortening of the length of the middle bench. When the length of the middle bench is 4 m (WC5), the final settlement of the tunnel roof is 8.5 cm, which is only 43.6% of that of WC1, and the shortening of the length of the middle bench can significantly reduce the final deformation of the tunnel. In addition, before the excavation of the middle bench, the difference in the settlement value of the tunnel arch for each condition is relatively small. The difference in tunnel deformation is mainly reflected in the middle bench excavation process. And the longer the length of the middle bench, the later the tunnel deformation converges. With the closure of the inverted arch, the tunnel primary support forms a whole structure, and the deformation gradually tends to stabilize.

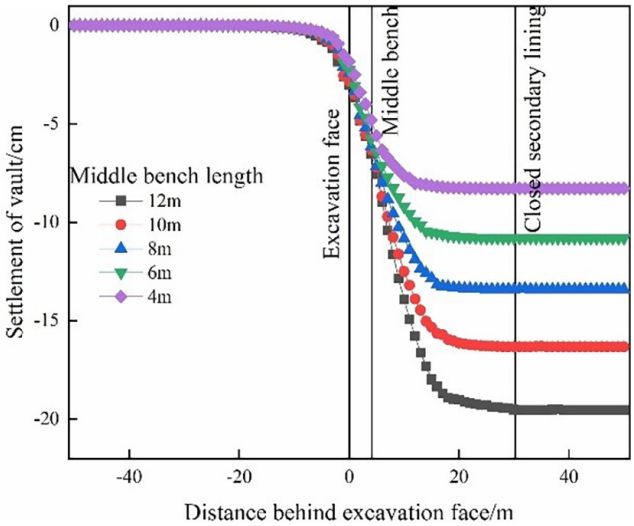


**Fig. 7** Longitudinal deformation curve of the tunnel

The tunnel arch settlement data of each excavation step from WC1 to WC5 were counted, as shown in Table 5. As the length of the middle bench decreases, the deformation of the upper and middle benches of the tunnel also decreases gradually, and the final settlement of the tunnel also decreases significantly. The ratio of the settlement of the tunnel roof of the upper and middle benches of the tunnel excavation to the total settlement of the vault for WC1~WC5 are 88.7%, 85.9%, 80.6%, 75.9% and 72.9%, respectively, which also show a decreasing trend. From Table 6, it can be seen that due to the soft rock stratum with hard top and soft bottom, the primary support structure erected after the excavation of the upper and middle benches of the tunnel was unable to resist the deformation and pressure of the surrounding rock, which was the main factor causing the vertical deformation of the tunnel.

Comparison of the tunnel roof settlement and arch waist horizontal convergence values for each working condition is shown in Fig. 8. With the shortening of the length of the middle step, the arch settlement value and horizontal convergence value basically show a linear decreasing trend.

**Table 6** Settlement statistics of tunnel roof

| WC | Settlement of tunnel roof/cm | | | Ratio of upper and middle benches settlement vault to total settlement/% |
|---|---|---|---|---|
| | Before excavation of the middle bench | Before excavation of the lower bench | Total settlement | |
| 1 | 6.5 | 17.3 | 19.5 | 88.7 |
| 2 | 6.2 | 14.0 | 16.3 | 85.9 |
| 3 | 5.7 | 10.8 | 13.4 | 80.6 |
| 4 | 5.3 | 8.2 | 10.8 | 75.9 |
| 5 | 4.9 | 6.2 | 8.5 | 72.9 |

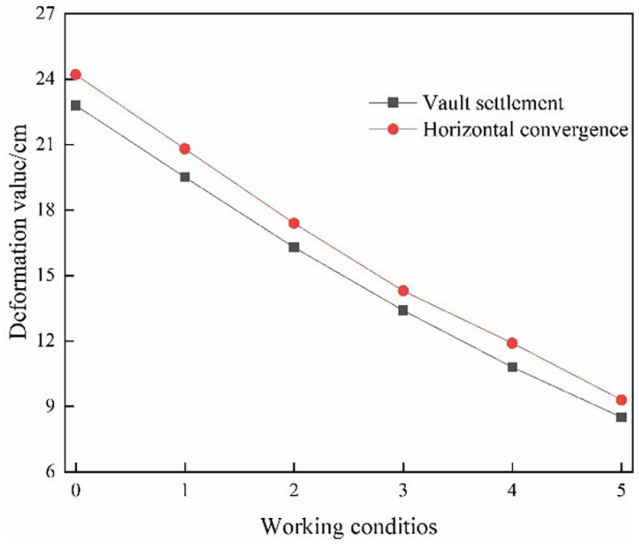


**Fig. 8** Comparison of tunnel deformation and convergence under each working condition

However, in actual construction, the middle bench is the main working surface for slagging and slurry spraying, and the length of the middle bench should consider the actual situation and should not be too short. In addition, as the tunnel arch waist is at the junction of soft and hard strata, the shear strength of surrounding rock changes abruptly there, resulting in the horizontal direction of surrounding rock extrusion into the cave. The horizontal convergence of the tunnel is slightly larger than the settlement value of the arch in all working conditions. Therefore, the tunnel support in the horizontal direction should be enhanced appropriately to reduce the horizontal convergence value of the tunnel.

By analyzing the contact pressure between the surrounding rock and the primary support, the mutual stress state between the surrounding rock and the primary support can be better judged. Since the FLAC software cannot directly extract the contact pressure between the surrounding rock and the primary support, the stress component of the monitoring points at the contact surface between the surrounding rock and the primary support is extracted. The stress direction is converted through Eq. (2). Fig. 9 shows the comparative radar map of the pressure distribution of surrounding rock for each working condition of the cave.

$$p = \sqrt{\left(\sigma_x + \tau_{yx} + \tau_{zx}\right)\cos\theta + \left(\sigma_y + \tau_{xy} + \tau_{zy}\right)\sin\theta} \qquad (2)$$

Where: $p$ is the pressure of the surrounding rock at the contact point; $\theta$ is the angle between the straight line and the horizontal axis of the monitoring point position at the perpendicular cave circumference.

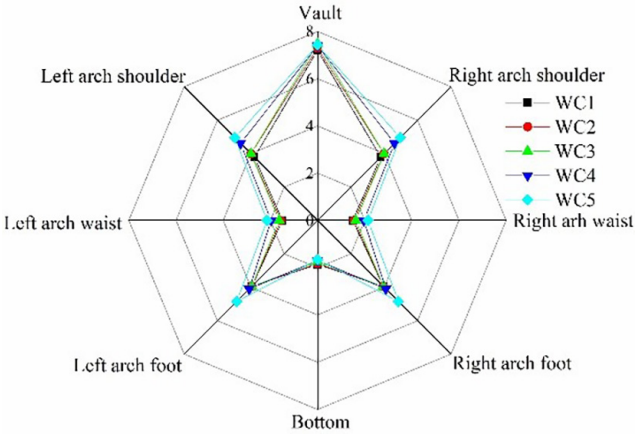


**Fig. 9** Distribution of surrounding rock pressure under each working condition (unit: 0.1 MPa)

From Fig. 9, it can be seen that the stress distribution around the tunnel cave for all conditions is in the butterfly shape. The pressure of the perimeter rock at the top of the arch is the largest, and the distribution of the arch waist and the bottom of the arch is the smallest. With the shortening of the length of the middle bench, the pressure of the tunnel roof is 0.72 MPa~0.74 MPa, and the pressure of the bottom is 0.05 MPa~0.08 MPa. Basically, it remains unchanged. When the length of the middle bench is 12 m (WC1), the pressure of the surrounding rock at the arch waist is the smallest, which is 0.03 MPa. With the shortening of the length of the middle bench, the pressure of the surrounding rock in the tunnel gradually increases. When the length of the middle bench is 4 m (WC5), the pressure of surrounding rock at the arch waist grows to 0.12 MPa. The distribution of rock pressure around the hole in each working condition shows that the shorter the length of the middle bench is, the more inadequate the release of rock stress around the hole is, and the greater the pressure of surrounding rock borne by the initial support is.

## 4 Optimization for anchor arrangement

According to the above numerical calculation results of different bench lengths, it can be seen that the excavation scheme of working condition 4, i.e. 4 m, 6 m and 2 m for the upper, middle and lower benches respectively, can be adopted. This scheme can ensure the deformation convergence requirements of the tunnel and also meet the actual construction conditions. However, in WC4, none of the anchors around the tunnel cave failed to pass through the plastic zone. At this time, the anchors can only play the role of reinforcing the surrounding rock, and cannot effectively play the suspension role of the anchors. Therefore, it is necessary to carry out research on the length of anchor rods and the arrangement around the tunnel.

### 4.1 Numerical calculation models for different anchor arrangement

Due to the soft rock in the lower part of the tunnel inverted arch, and the numerical calculation shows that the radius of the plastic zone in this area is large. Therefore, the full-section anchors are used for reinforcement, and the anchor arrangement is in the form of plum blossom piles, with a ring spacing of 1 m and an axial spacing of 0.6 m. According to the size of the depth of the plastic zone and the deformation convergence of the tunnel circumference in WC4, different lengths of anchors are set up for reinforcement cases, as shown in Table 7. The numerical simulation model of tunnel excavation is the same as that of WC4, and only the anchor arrangement around the tunnel is changed.

### 4.2 Analysis of calculation results

The depth of the plastic zone around the tunnel from WC I to WC IV was extracted, as shown in Table 8 and Fig. 10. From Table 8 and Fig. 10, it can be seen that with the increase of the anchor length, the depth of the plastic zone at each point around the hole shows a decreasing trend. And the depth of the plastic zone in the arch waist is the largest in each working condition. When 3 m anchor rods (WC I) are arranged in the whole section around the cave, the depth of plastic zone at the arch waist is the largest, which is 6.4 m, far exceeding the length of anchor rods. At this time, the role played by the anchors around the hole is small. When the length of anchor rods around the tunnel is 4.5 m (WC II), except for the arch top, the rest of the position of anchor rods are not beyond the scope of the plastic zone. The depth of the plastic zone around the tunnel is slightly reduced, and the roles played by the anchors in

**Table 7** Numerical simulation working condition design of anchor arrangement

| WC | Anchor length/m | | | |
|---|---|---|---|---|
| | Upper bench | Middle bench | Lower bench | Inverted arch |
| I | 3 | 3 | 3 | 3 |
| II | 4.5 | 4.5 | 4.5 | 4.5 |
| III | 6 | 6 | 6 | 6 |
| IV | 4.5 | 6 | 6 | 4.5 |

**Table 8** Depth of the plastic zone of different anchor arrangement

| WC | Depth of the plastic zone/m | | | | |
|---|---|---|---|---|---|
| | Vault | Arch shoulder | Arch waist | Arch foot | Inverted arch |
| I | 4.3 | 5.1 | 6.4 | 6.2 | 4.8 |
| II | 4.1 | 4.9 | 6.1 | 5.9 | 4.5 |
| III | 3.8 | 4.5 | 5.4 | 5.3 | 3.9 |
| IV | 3.9 | 4.5 | 5.5 | 5.4 | 4.1 |

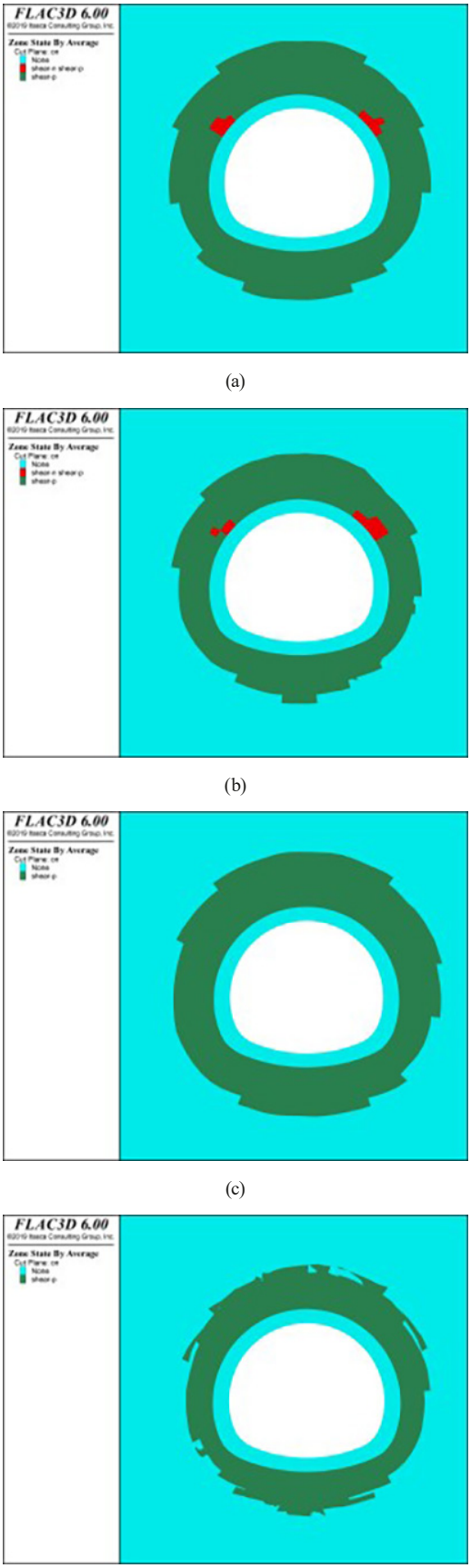


(a) (b) (c) (d)

**Fig. 10** Plastic zone of different anchor arrangement: (a) WC I, (b) WC II, (c) WC III, (d) WC IV

WC II and WC I are basically the same. When 6 m anchors (WC III) are arranged in the whole section, the depth of the plastic zone of the tunnel is significantly reduced. Compared with WC I, the depth of the plastic zone around the hole is reduced by 11.6%~18.8%, and the depth of the plastic zone at the bottom of the arch is reduced most obviously. Since the depth of the plastic zone at the top of the arch and the bottom of the arch is smaller for each working condition. Therefore, the length of the anchor rods of the upper bench and the inverted arch was optimized again to 4.5 m (WC IV) in order to reduce the cost of support. From Table 8 and Fig. 10, it can be seen that the depth of the plastic zone of the optimized tunnel changes less compared with WC III, and the length of the anchor rods all pass through the range of the plastic zone, so it is more reasonable to adopt the anchor rod arrangement of WC IV.

Since the depth of plastic zone at the arch waist is maximum in WC I~WC IV, the size of the anchor rod axial force distribution along the length at the arch waist will be extracted and analyzed. Among them, the spacing of the monitoring points of the axial force on the anchor rods is 0.5 m, and the distribution of the axial force of the anchor rods along the length is shown in Fig. 11, which stipulates that the anchor rods are positive in tension and negative in compression. In WC I and WC II, the axial force of the anchor rods along the length is small. And the negative value appeared in the range of 2 m close to the surrounding rock. Because the length of the anchor rod does not exceed the depth of the plastic zone, and the surrounding rock in the plastic zone is displaced to the cave compared with the anchor rod, resulting in local compression of the anchor rod, which generates pressure. The axial force of the anchor rod in WC III and WC IV is peaked at a distance of 5 m from the waist of the arch, which is 70.6 kN and 71.8 kN, and this position is basically in the elastic-plastic junction range of the tunnel. As the deformation of the surrounding rock in the elastic zone is small, the surrounding rock deforms outward relative to the anchor rods. And the surrounding rock in the plastic loosening zone deforms to the tunnel relative to the anchor rods, so the peak of the anchor rod axial force is formed at the elastic-plastic junction. From Fig. 11, it can be seen that when the length of anchor rods exceeds the depth of the plastic zone of the tunnel, it can better play its reinforcing and suspending roles, and improve the self-stabilizing ability of the surrounding rock.

Comparison of the final values of deformation convergence around the hole for each condition is shown in Fig. 12. With the increase of the anchor length, the tunnel roof settlement and horizontal convergence value both show a decreasing trend. And the value of tunnel roof is slightly smaller than the horizontal convergence value. The values of vault settlement and horizontal convergence in WC I (full section 3 m anchor) are 10.8 cm and 11.5 cm respectively. Compared with WC4 (elevation arch without anchor) in Section 3, it is basically the same, and only arranging the full-section 3 m short anchors can't reduce the deformation convergence of the cave periphery. In WC III, compared with WC I, the values of vault settlement and horizontal convergence are reduced by 12.0% and 12.2% respectively. Compared with WC III, the change of settlement value and horizontal convergence value is smaller, and the appropriate shortening of the length of the vault anchor can reduce the cost of support as well as the difficulty of construction.

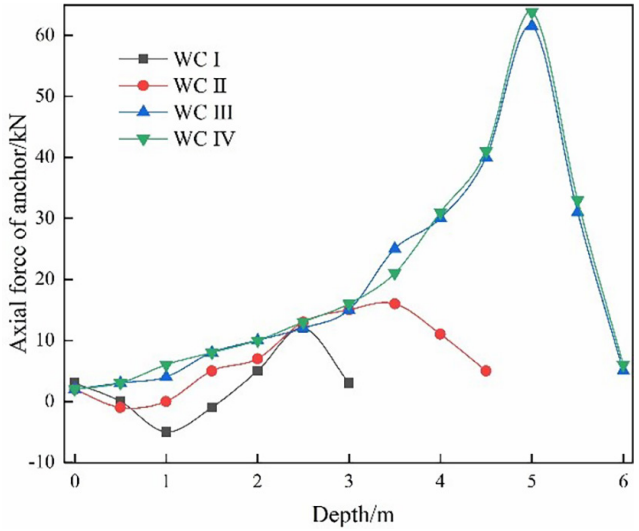


**Fig. 11** Axial force of anchor rod

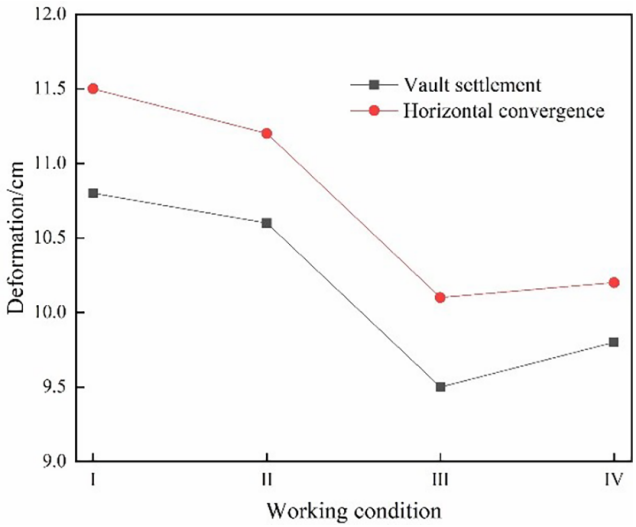


**Fig. 12** Final deformation value of each working condition

In summary, considering the support cost, construction difficulty and structural stability, it is more reasonable to take the length of anchor rods of the optimized upper bench, middle bench, lower bench and inverted arch as 4.5 m, 6 m, 6 m and 4.5 m respectively.

## 5 Specific construction optimization measures and field applications

### 5.1 Construction optimization measures

The construction measures optimized based on numerical simulation results and actual site conditions are as follows:

1. Shorten the advance length of benches. Optimize the length of the upper bench, middle bench and lower bench to 4 m, 6 m and 2 m respectively. In addition, the inverted arch is applied immediately after the lower bench, so that the tunnel primary support can be closed into a ring as early as possible, and the overall rigidity of the primary support can be improved. NATM method of bench excavation in the middle, the lower bench of the left and right excavation alternately, shall not make the two sides of the primary support arch foot at the same time exposed.
2. Adjust the anchor arrangement. Setting full section anchor reinforcement program, the anchor adopts the form of plum blossom pile arrangement, axial spacing 0.6 m, ring spacing 1 m. The length of the upper bench and inverted arch anchor is 4.5 m, the length of the anchor in the middle and lower bench is 6 m. The anchor selects the steel pipe, the front end of which is made into a sharp cone, and the tail is welded with ∅8 mm steel bar as a reinforcing hoop. And in the wall of the pipe every 15 cm staggered drilling eyes, eye diameter of 8 mm, anchor should ensure that the end of the anchor welding and timely grouting.
3. Optimize the excavation method. The upper bench and the middle bench of strongly weathered granite using surface blasting technology, but as far as possible to reduce the blasting vibration on the lower soft rock layer disturbance. After excavation of the middle bench, local grouting is carried out to reinforce the soft surrounding rock at the arch foot, so that the arch foot has reliable support. The lower bench of fully weathered granite using micro-step mechanical excavation, the left and right sides from the alternating staggered excavation. This cannot only reduce the amount of excavation and timely support, but also provide a support point or backfill counterpressure in the event of large deformation of the side wall. As the surrounding rock in the upper and middle benches is slightly better, the excavation footage can be increased appropriately according to the deformation of the tunnel. But the lower bench excavation footage needs to be strictly controlled for 1 m, to prevent the primary support structure deformation is too large and local subsidence disaster.
4. Enhance the monitoring means. Due to the tunnel through the upper hard and lower soft stratum when the risk is greater, and the deformation of the tunnel convergence often lags behind the changes in the surrounding rock pressure. Therefore, on the basis of tunnel deformation monitoring, the surrounding rock pressure and primary support force should be continuously monitored, so as to reserve time for tunnel disaster disposal.

### 5.2 Field applications

The optimisation measures in Section 4.1 were applied to the actual Magu Tunnel project. Fig. 13 shows the comparison of the deformation of the tunnel before and after the optimisation. As can be seen from Fig. 13, the application of the optimised construction scheme is very effective in controlling the deformation of the tunnel.

As can be seen from Fig. 13, the final settlement of the tunnel roof after optimisation is 11.3 cm, which is a reduction of 50.5% compared to the pre-optimisation vault settlement value. The optimised construction scheme can significantly reduce the tunnel deformation convergence. In addition, the settlement of the tunnel roof before the excavation of the lower bench is significantly smaller than the pre-optimised settlement due to the reduction of the length of the middle bench and the application of

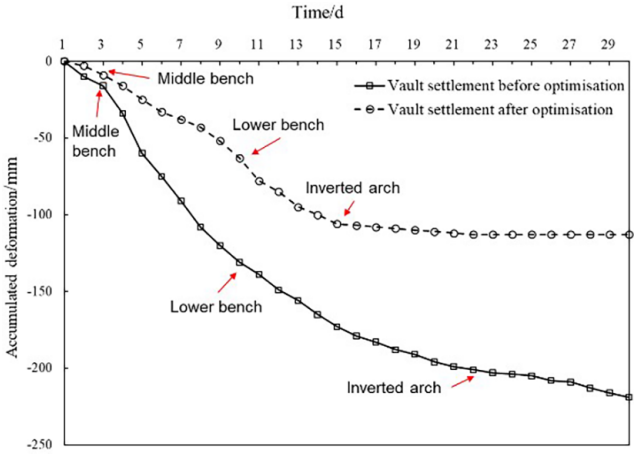


**Fig. 13** Comparison of the tunnel roof settlement before and after optimization

anchors. The deformation of the tunnel after excavation of the lower bench is still slightly larger in the optimised construction plan. However, due to the shorter length of the lower bench and the inverted arch, with the closure of the inverted arch, the deformation of the tunnel quickly reaches a convergence state, effectively controlling the deformation of the tunnel's primary support structure, and guaranteeing the safety of the primary support structure.

## 6 Conclusions

In this paper, for the Mengmeng Expressway Magu Tunnel in Yunnan Province, which crosses the upper hard and lower soft stratum, the deformation is large and the construction safety risk is big. The bench length and the anchor arrangement are optimised by the numerical simulation. The following conclusions are drawn:

1. Influenced by the special stratum of upper hard and lower soft strata, the pressure relief of surrounding rock is most obvious at the arch waist position. The pressure of surrounding rock is butterfly-shaped distribution and gradually increases with the decrease of the length of the middle bench. The difference in tunnel deformation mainly occurs after the excavation and support of the middle bench. In addition, under the influence of the soft and hard stratum junction at the foot of the middle bench, the shear strength of the surrounding rock at this position changes abruptly, resulting in local unloading and large horizontal convergence.
2. With the shortening of the length of the middle bench, the deformation convergence of the tunnel is gradually reduced. However, as the main working plane of construction, the middle bench should not be too short. Anchor rods play the role of reinforcing surrounding rock and suspension in tunnel support. When the length of anchor rods does not pass through the depth of plastic zone, the axial force of anchor rods is low, and the deformation control effect on the tunnel is weak. When the anchor length passes through the depth of the plastic zone, the peak axial force is generated near the junction range of the plastic zone and the elastic zone, which can play a better role in reinforcing the surrounding rock and reduce the deformation convergence of the tunnel.
3. Optimise the length of the upper, middle and lower benches and inverted arches to 4 m, 6 m, 2 m and 2 m respectively, and the excavation footage is 1 m, and lay out the full-section anchor rods around the hole, with the length of the upper and inverted arches of 4.5 m, and the length of the middle and lower benches of 6 m, which can significantly reduce the deformation convergence of the tunnel after the optimisation of the construction plan. Compared with the pre-optimised vault settlement value, it was reduced by 50.5%. The optimised excavation support scheme can not only control the occurrence of local subsidence or toppling disaster of surrounding rock, but also ensure a safe and efficient construction environment.

## Conflict of interest

The author order of this paper has been unanimously agreed by all authors, and there is no conflict of interest between them.

## Acknowledgement

The related work of this study was supported by Yunnan Provincial Department of Transportation Scientific Research Project (NO. 2022028).

## References

[1] Wu, K., Song, J., Zheng, X., Zhao, N., Shao, Z., Chu, Z. "The deformation coordination-dominated design of yielding supports applied in large deformation tunnels", Acta Geotechnica, 19(5), pp. 2499–2513, 2024. https://doi.org/10.1007/s11440-024-02264-5

[2] Li, G., Zhu, C., Hongliang, L., Tang, S., Du, K., Wu, C. Z. "Energy balance support method in soft rock tunnel with energy absorbing anchor cable", Tunnelling and Underground Space Technology, 141, 105380, 2023. https://doi.org/10.1016/j.tust.2023.105380

[3] Xu, J., Xie, X., Tang, G., Zhou, B., Xu, D., Huang, Y. "A new adaptive compressible element for tunnel lining support in squeezing rock masses", Tunnelling and Underground Space Technology, 137, 105124, 2023. https://doi.org/10.1016/j.tust.2023.105124

[4] Tian, Y., Shu, X., Tian, H., He, L., Jin, Y., Huang, M. "Effect of horizontal stress on the mesoscopic deformation and failure mechanism of layered surrounding rock masses in tunnels", Engineering Failure Analysis, 148, 107226, 2023. https://doi.org/10.1016/j.engfailanal.2023.107226

[5] Fan, X., Juang, C. H., Wasowski, J., Huang, R., Xu, Q., Scaringi, G., van Westen, C. J., Havenith, H.-B. "What we have learned from the 2008 Wenchuan Earthquake and its aftermath: A decade of research and challenges", Engineering Geology, 241, pp. 25–32, 2018. https://doi.org/10.1016/j.enggeo.2018.05.004

[6] Wu, K., Shao, Z., Jiang, Y., Zhao, N., Qin, S., Chu, Z. "Determination of Stiffness of Circumferential Yielding Lining Considering the Shotcrete Hardening Property" Rock Mechanics and Rock Engineering, 56(4), pp. 3023–3036, 2023. https://doi.org/10.1007/s00603-022-03122-0

[7] Sun, H., Gao, Y., Fang, Z., Chen, Y., Yang, Y. "Full-Scale Rotary Cutting Experimental Study and Development of Prediction Formulas for TBM Cutting Force", Arabian Journal for Science and Engineering, 48(10), pp. 13353–13376, 2023. https://doi.org/10.1007/s13369-023-07805-w

[8] Tran Manh, H., Sulem, J., Subrin, D., Billaux, D. "Anisotropic time-dependent modeling of tunnel excavation in squeezing ground", Rock Mechanics and Rock Engineering, 48(6), pp. 2301–2317, 2015. https://doi.org/10.1007/s00603-015-0717-y

[9] Li, Y., Zhang, D., Fang, Q., Yu, Q., Xia, L. "A physical and numerical investigation of the failure mechanism of weak rocks surrounding tunnels", Computer and Geotechics 61, pp. 292–307, 2014. https://doi.org/10.1016/j.compgeo.2014.05.017

[10] Wu, H., Fan, F., Yang, X., Wang, Z., Lai, J., Xie, Y. "Large Deformation Characteristics and Treatment Effect for Deep Bias Tunnel in Broken Phyllite: A Case Study",Engineering Failure Analysis, 135, 106045, 2022. https://doi.org/10.1016/j.engfailanal.2022.106045

[11] Liu, W., Chen, J., Luo, Y., Chen, L., Shi, Z., Wu, Y. "Deformation Behaviors and Mechanical Mechanisms of Double Primary Linings for Large-Span Tunnels in Squeezing Rock: A Case Study", Rock Mechanics and Rock Engineering, 54(5), pp. 2291–2310, 2021. https://doi.org/10.1007/s00603-021-02402-5

[12] Xu, C., Xia, C. "A new large strain approach for predicting tunnel deformation in strain-softening rock mass based on the Generalized Zhang-Zhu strength criterion", International Journal of Rock Mechanics and Mining Sciences, 143, 104786, 2021. https://doi.org/10.1016/j.ijrmms.2021.104786

[13] Li, G., Ma, F., Guo, J., Zhao, H., Liu, G. "Study on deformation failure mechanism and support technology of deep soft rock roadway", Engineering Geology, 264, 105262, 2020. https://doi.org/10.1016/j.enggeo.2019.105262

[14] Cao, C., Shi, C., Lei, M., Yang, W., Liu, J. "Squeezing failure of tunnels: A case study, Tunnelling and Underground Space Technology, 77, pp. 188–203, 2018. https://doi.org/10.1016/j.tust.2018.04.007

[15] Zhigang, T., Fei, Z., Hongjian, W., Haijiang, Z., Yanyan, P. "Innovative constant resistance large deformation bolt for rock support in high stressed rock mass", Arabian Journal of Geosciences, 10(15), 341, 2017. https://doi.org/10.1007/s12517-017-3127-5

[16] Sun, Z., Zhang, D., Hou, Y., Huangfu, N., Li, M., Guo, F. "Support Countermeasures for Large Deformation in a Deep Tunnel in Layered Shale with High Geostresses", Rock Mechanics and Rock Engineering, 56(6), pp. 4463–4484, 2023. https://doi.org/10.1007/s00603-023-03297-0

[17] Li, Z., Ma, E., Lai, J., Su, X. "Tunnel deformation prediction during construction: An explainable hybrid model considering temporal and static factors", Computers and Structures, 294, 107276, 2024. https://doi.org/10.1016/j.compstruc.2024.107276

[18] Chen, Z., He, C., Xu, G., Ma, G., Yang, W. "Supporting mechanism and mechanical behavior of a double primary support method for tunnels in broken phyllite under high geo-stress: a case study", Bulletin of Engineering Geology and the Environment, 78(7), pp. 5253–5267, 2019. https://doi.org/10.1007/s10064-019-01479-1

[19] Oke, J., Vlachopoulos, N., Diederichs, M."Improvement to the Convergence-Confinement Method: Inclusion of Support Installation Proximity and Stiffness", Rock Mechanics and Rock Engineering, 51(5), pp. 1495–1519, 2018. https://doi.org/10.1007/s00603-018-1418-0

[20] Liu, W., Chen, J., Luo, Y., Chen, L., Zhang, L., He, C., Shi, Z., Xu, Z., Zhu, H., Hu, T., Dong, F. "Long-term stress monitoring and in-service durability evaluation of a large-span tunnel in squeezing rock", Tunnelling and Underground Space Technology, 127, 104611, 2022. https://doi.org/10.1016/j.tust.2022.104611

[21] Yang, Y., Meng, L., Zhang, T. "Full Anchor Cable Support Mechanism and Application of Roadway with Thick Soft Rock Mass Immediate Roof", Applied Sciences, 13(12), 7148, 2023. https://doi.org/10.3390/app13127148

[22] Cai, W., Zhu, H., Liang, W. "Three-dimensional tunnel face extrusion and reinforcement effects of underground excavations in deep rock masses", International Journal of Rock Mechanics and Mining Sciences, 150, 104999, 2022. https://doi.org/10.1016/j.ijrmms.2021.104999